

Entanglement enhanced phase sensitive Raman scattering in atomic vapors

Chun-Hua Yuan¹, L. Q. Chen¹, Z. Y. Ou^{1,2,*}, and Weiping Zhang^{1†}

¹Quantum Institute for Light and Atoms, Department of Physics,
East China Normal University, Shanghai 200062, P. R. China

²Department of Physics, Indiana University-Purdue University Indianapolis,
402 North Blackford Street, Indianapolis, Indiana 46202, USA

(Dated: December 10, 2018)

We theoretically present a new method to enhance Raman scattering by injecting seeded light field that is entangled with the initially prepared atomic spin wave. From theoretical analysis and numerical calculation, we find that strong Raman scattering can be obtained. Different from other enhancement mechanisms, the entanglement enhanced Raman scattering is phase sensitive. Such an enhancement method in Raman scattering may have practical applications in quantum information, nonlinear optics and optical metrology due to its simplicity.

PACS numbers: 42.65.Dr, 42.50.Gy, 42.25.Bs

I. INTRODUCTION

The cooperative spontaneous emission of radiation (superradiance) from an ensemble was first introduced by Dicke in 1954 [1], where an atomic ensemble exhibited enhanced coupling to a single electromagnetic mode. Superradiance was initially for sample dimensions R much smaller than the wavelength λ of the resonant transition [1]. However, the case in the opposite limit $R \gg \lambda$ has attracted extensive research [2–10] because in quantum optics the sample is usually large compared to λ . So in this case, there is no macroscopic dipole moment because the dipole-dipole interaction can be neglected and the superradiance will not appear according to standard argument. To have enhancement in the limit of $R \gg \lambda$ the quantum coherence and interference must play a role. In this case, the medium has an active role in nonlinear optical processes [11], in contrast to the traditional nonlinear optics where the medium has a rather passive role [12]. Recently, our group observed an enhanced Raman scattering effect by a prebuilt atomic spin wave [8, 9]. The subsequent theoretical analysis showed that the initial atomic spin wave prepared by a spontaneous Raman scattering has a spatial distribution which leads to an enhanced scattering of the second Raman write field [13]. The flipped atoms act as seeds to the second Raman process which amplifies all the way through the atomic medium.

In this paper, based on our previous work [8, 9, 13], we propose a new enhancement scheme for Raman scattering, termed entanglement enhanced Raman scattering (EERS). In our scheme, the first pump field leads to spontaneous emission of the Stokes field that is subsequently used as a seeded signal with the pump field together input the atomic ensemble again to generate a second Stokes pulse. In the Raman scattering process, the numbers of Stokes photons and collective atomic spin excitations (also called atomic spin wave) are equal. Therefore, a two-mode squeezed state $|\psi\rangle = \sum_{n=0}^{\infty} c_n |n\rangle_{\text{photon}} |n\rangle_{\text{spin}}$ is generated between the Stokes field and the collective atomic spin excitation [14–16]. The quantum cor-

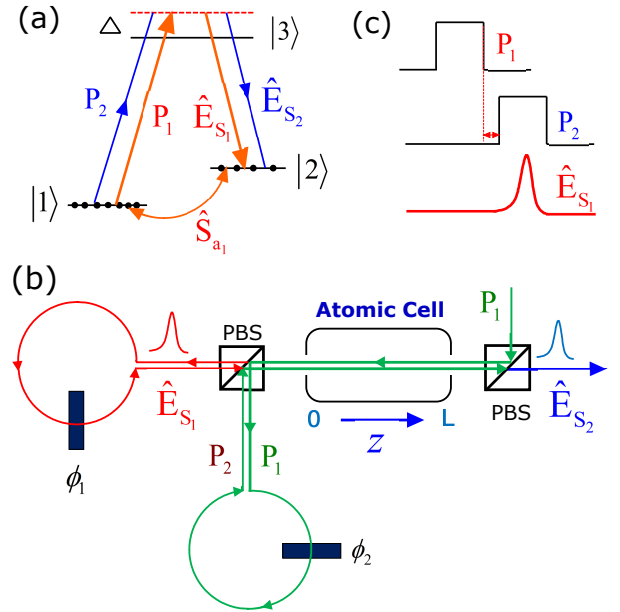


FIG. 1: (Color online) (a) The schematic diagram of three-level atoms. P_1 , P_2 : pump fields; \hat{E}_{S_1} , \hat{E}_{S_2} : the generated Stokes fields; Δ : the detuning; \hat{S}_{a_1} : initial prepared spin wave. (b) Experimental schematic. The pump field (denoted by P_1) leads to spontaneous Raman scattering \hat{E}_{S_1} and flipped atomic spins \hat{S}_{a_1} . After a short delay, the leak write field (denoted by P_2) with the generated Stokes field \hat{E}_{S_1} are together input to the atomic medium again. The entanglement of the light \hat{E}_{S_1} and initially prepared spin wave \hat{S}_{a_1} will enhance the intensity of second Raman scattering \hat{E}_{S_2} . The two circles are delays. PBS: polarization beam splitter; ϕ_1 , ϕ_2 : phase shifts. (c) The time sequence for different fields.

related atom-photon pair very analogous to twin light beam generation in an optical parametric process, and it is also an EPR-type entanglement state [17–20]. The entanglement of seeded light and initially prepared spin wave (IPSW) leads to generate enhanced Raman scattering. Our enhancement mechanism is different from the

quantum-entanglement-initiated super Raman scattering [10], where the entanglement referred to the initial state of atomic ensemble. Our enhancement mechanism is a combination of two types of enhancement mechanisms—seeded light mechanism, spin wave based on mechanism. But this combination is a coherent sum, not an incoherent sum. I.e., not sum the intensities from the two mechanisms, but a sum of the probability amplitudes contributed from the two mechanisms because the seeded light and the spin wave are entangled quantum mechanically. The phase sensitive effect in the new scheme is a reflection of the probability amplitude addition.

Our article is organized as follows. In Sec. II, to describe the generation of EERS conveniently, an idealized few-mode model with no spatial propagation effects is first used. Then a proper model involving spatial propagation is given. In Sec. III, we numerically calculate the intensities of the different enhanced mechanism and compared them each other, which shows that the intensity generated by the correlation enhanced mechanism is the largest of three cases. Finally, we conclude with a summary of our results.

II. ENHANCED RAMAN SCATTERING

The energy level diagram and the experimental schematic are shown in Fig. 1(a) and 1(b), respectively. The first pump field leads to spontaneous emission of the Stokes field that is subsequently used as a feed signal generating a second Stokes impulse. It should be noted that under such conditions the feed field and the polarization field in the medium are correlated, this correlation leads to new effects like enhanced emission. Firstly, to describe the physics of this process, a simple mode involving no spatial propagation is introduced.

A. Few-mode model

Now, we first use a linear amplifier theory to describe the process of enhanced Raman scattering. If atomic saturation and dephasing as well as spatial effects can be ignored, the generated fields by the Raman system are [21]

$$\hat{A}_{S_1} = G_1 \hat{A}_{S_{in}} + g_1 \hat{B}_{a_{in}}^\dagger, \quad (1)$$

$$\hat{B}_{a_1}^\dagger = G_1^* \hat{B}_{a_{in}}^\dagger + g_1^* \hat{A}_{S_{in}}, \quad (2)$$

where \hat{A}_S and \hat{B}_a are is a electromagnetic field operator and a collective atomic field operator, respectively. G_1 and g_1 are gain coefficients with the relation $|G_1|^2 - |g_1|^2 = 1$. At $t = 0$, both fields $\hat{A}_{S_{in}}$ and $\hat{B}_{a_{in}}$ are in their vacuum states: no photons in the Stokes field and no atoms in state $|2\rangle$. After the Raman process, the output intensity of Stokes field S_1 is given by

$$I_{S_1} = \frac{\hbar\omega_{S_1}c}{L} \langle \hat{A}_{S_1}^\dagger \hat{A}_{S_1} \rangle = I_{\text{spon}_1}. \quad (3)$$

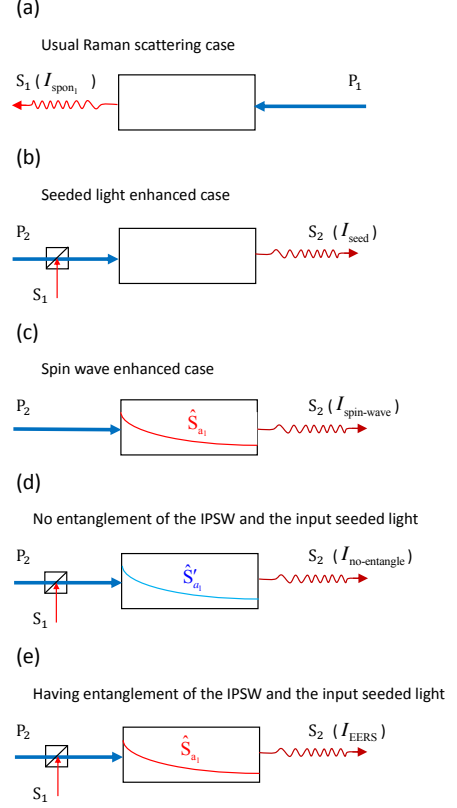


FIG. 2: (Color online) (a)-(e) Different Raman scattering mechanisms. (c)-(e) The seeded light S_1 is entangled with the IPSW \hat{S}_{a_1} , not entangled with another IPSW \hat{S}'_{a_1} .

And the Stokes photons and excited-state atoms are created in equal numbers $\langle \hat{A}_{S_1}^\dagger \hat{A}_{S_1} \rangle = \langle \hat{B}_{a_1}^\dagger \hat{B}_{a_1} \rangle = |g_1|^2$. For such a two-mode squeezed state $|\psi\rangle = \sum_{n=0}^{\infty} c_n |n\rangle_{\text{photon}} |n\rangle_{\text{spin}}$ between the Stokes field and the collective atomic spin excitation, in the Schrödinger picture the entangled state (unnormalized) is [14]

$$\Psi(\hat{q}_{S_1}, \hat{q}_{a_1}) = e^{-[(G_1 \hat{q}_{S_1} - g_1 \hat{q}_{a_1})^2 + (G_1 \hat{q}_{a_1} - g_1 \hat{q}_{S_1})^2]/2}, \quad (4)$$

where $\hat{A}_{S_1} = (\hat{q}_{S_1} + i\hat{p}_{S_1})/\sqrt{2}$, $\hat{B}_{a_1} = (\hat{q}_{a_1} + i\hat{p}_{a_1})/\sqrt{2}$, and $[\hat{q}_j, \hat{p}_k] = i\delta_{jk}$. This pure state describes strong correlations both in excitation numbers and in phase.

After the Stokes field S_1 undergoing a ϕ -phase shift with the leak pump field as the input inject the Raman system again, the generated fields are

$$\hat{A}_{S_2} = G_2 \hat{A}_{S_1} e^{i\phi} + g_2 \hat{B}_{a_1}^\dagger, \quad (5)$$

$$\hat{B}_{a_2}^\dagger = G_2^* \hat{B}_{a_1}^\dagger + g_2^* \hat{A}_{S_1} e^{i\phi}, \quad (6)$$

where $|G_2|^2 - |g_2|^2 = 1$. Now, the initial fields \hat{A}_{S_1} and \hat{B}_{a_1} are not in vacuum states, and the output intensity of Stokes field S_2 is given by

$$\begin{aligned} I_{S_2} &\equiv I_{\text{EERS}} = \frac{\hbar\omega_{S_2}c}{L} \langle \hat{A}_{S_2}^\dagger \hat{A}_{S_2} \rangle \\ &= I_{\text{spon}_2} + \text{Tm}_{\text{seed}} + \text{Tm}_{\text{spin-wave}} + \text{Tm}_{\text{EPR}}, \end{aligned} \quad (7)$$

where

$$\begin{aligned}
I_{\text{spont}_2} &= \frac{\hbar\omega_{S_2}c}{L} |g_2|^2, \\
\text{Tm}_{\text{seed}} &= \frac{\hbar\omega_{S_2}c}{L} |G_2|^2 \langle \hat{A}_{S_1}^\dagger \hat{A}_{S_1} \rangle, \\
\text{Tm}_{\text{spin-wave}} &= \frac{\hbar\omega_{S_2}c}{L} |g_2|^2 \langle \hat{B}_{a_1}^\dagger \hat{B}_{a_1} \rangle, \\
\text{Tm}_{\text{EPR}} &= \frac{\hbar\omega_{S_2}c}{L} [G_2 g_2^* e^{i\phi} \langle \hat{B}_{a_1} \hat{A}_{S_1} \rangle + \text{H.c.}]. \quad (8)
\end{aligned}$$

The structure of Raman equations (1)-(2) and (5)-(6) does not change, but the different initial conditions lead to Raman scattering enhancement, which are seen from equations (3) and (7). The intensity I_{spont_2} describes the intensity of Stokes field when only the field P_2 drives the ensemble and without any other enhancement mechanisms existing. The terms Tm_{seed} , $\text{Tm}_{\text{spin-wave}}$, and Tm_{EPR} appeared from the seed, spinwave, and entanglement enhancement mechanisms, respectively.

Different Raman scattering cases are summarized in Fig. 2. When either seeded light or spin wave enhancement mechanism does work, the corresponding enhanced terms Tm_{seed} or $\text{Tm}_{\text{spin-wave}}$ will appear. Then the intensities of the two cases are written as

$$I_{\text{seed}} = I_{\text{URS}} + \text{Tm}_{\text{seed}}, \quad (9)$$

$$I_{\text{spin-wave}} = I_{\text{URS}} + \text{Tm}_{\text{spin-wave}}. \quad (10)$$

which are shown in Fig. 2(b) and Fig. 2(c), respectively. The spin wave enhancement mechanism has been studied by us in theory and on experiment [8, 9, 13], which is depend on the spatial distribution of the initial prepared spin wave and can not describe only using the simple few-mode model. When above two mechanisms have been put into effect simultaneously but independently shown in Fig. 2(d), the enhanced effects generated by different mechanisms are incoherent combining and only the intensities from two enhancement mechanisms sum. Therefore the intensity of this without entanglement case is given by

$$I_{\text{no-entangle}} = I_{\text{URS}} + \text{Tm}_{\text{seed}} + \text{Tm}_{\text{spin-wave}}. \quad (11)$$

However, for EERS case shown in Fig. 2(e), it is a coherent summation, i.e., a sum of the probability amplitudes contributed from the two mechanisms. Therefore the intensity of Stokes field I_{EERS} of Eq. (7) can be enhanced not only from the addition of the terms of two enhancement mechanisms, but also from the entanglement of the injected Stokes field and the IPSW. To compare the intensity of these enhanced cases, we firstly consider a simple case, let G and g are real and $G_1 = G_2 = G$; $g_1 = g_2 = g$. Therefore, these intensities are rewritten as

$$\begin{aligned}
I_{\text{spont}_2} &= \frac{\hbar\omega_{S_2}c}{L} g^2; \quad I_{\text{seed}} = \frac{\hbar\omega_{S_2}c}{L} (g^2 + G^2 g^2); \\
I_{\text{spin-wave}} &= \frac{\hbar\omega_{S_2}c}{L} G^2 g^2; \quad I_{\text{no-entangle}} = 2 \frac{\hbar\omega_{S_2}c}{L} G^2 g^2; \\
I_{\text{EERS}} &= 2 \frac{\hbar\omega_{S_2}c}{L} G^2 g^2 (1 + \cos \phi). \quad (12)
\end{aligned}$$

Obviously, the EERS enhanced case is phase sensitive and the Stokes intensity is dependent on the relative phase of the pump field and seeded light, which had not been studied in Raman scattering. For a certain ϕ , such as $\phi = 0$ or 2π , the intensity of the EERS enhanced case is the highest of them. Under this conditions the intensity relation of them is $I_{\text{EERS}} = 2 I_{\text{no-entangle}} = 4 I_{\text{spin-wave}} \approx 4 I_{\text{seed}} \gg I_{\text{spont}_2}$.

B. Involving Spatial Propagation

In this section, we shall analyze the enhanced Raman scattering using a proper model [22] involving the spatial propagation. Firstly, optical pumping prepares all atoms in their ground hyperfine state $|1\rangle$, then an off-resonant pump field P_1 is applied to the atomic ensemble, inducing spontaneous Raman scattering $\hat{\mathcal{E}}_{S_1}$ and flipped atomic spins \hat{S}_{a_1} are created. Assume the pump field (Ω_{P_1}) corresponding to a focused beam and the Fresnel number $\mathfrak{F} = A/\lambda_{S_1} L$ (A cross-sectional area, L cell length) is of the order of unity, then only a single transverse spatial mode contributes strongly to emission along the direct of the pump field (Ω_{P_1}). Therefore the above mode can be simplified as a one-dimensional model, the propagating quantized Stokes field $\hat{\mathcal{E}}_{S_1}$ obeys the equation of motion [22]

$$\begin{aligned}
(\partial_t + c\partial_z)\hat{\mathcal{E}}_{S_1}(z, t) &= i\chi_1 \hat{S}_{a_1}^\dagger, \\
\partial_t \hat{S}_{a_1}^\dagger &= -\Gamma_{S_1} \hat{S}_{a_1}^\dagger - i\chi_1^* \hat{\mathcal{E}}_{S_1} + \hat{F}_{S_1}^\dagger, \quad (13)
\end{aligned}$$

where $\chi_1(z, t) = g\sqrt{N}\Omega_{W_1}(z, t)/\Delta$, $\Gamma_{S_1} = \gamma_{S_1} - i\delta_{L_1}$, $\gamma_{S_1} = \gamma_{S_0} + \gamma_1 |\Omega_{W_1}|^2/\Delta^2$, $\hat{S}_{a_1} = \sqrt{N}\tilde{\sigma}_{12} e^{-i\Delta kz}$ the spin wave operator, and $\delta_{L_1} = |\Omega_{W_1}|^2/\Delta$ is the AC Stark shift, and $\Delta k = k_{W_1} - k_{S_1}$, γ_{S_0} the coherence ($\tilde{\sigma}_{12}$) decay rate, γ_1 the decay rates of the excited state $|3\rangle$ to states $|1\rangle$ and $|2\rangle$ (assuming $\gamma_{31} = \gamma_{32} = \gamma_1$). $\hat{F}_{S_1}^\dagger$ is the Langevin noise operator and $\langle \hat{F}_{S_1}^\dagger(z, t) \hat{F}_{S_1}^\dagger(z', t') \rangle = 2\gamma_{S_1} V \delta(z - z') \delta(t - t')$.

After the write field left the atomic medium, the leak pump field (denoted by P_2 , $\Omega_{P_2} = \eta_P \Omega_{P_1}$) with the generated Stokes field $\eta_S \hat{\mathcal{E}}_{S_1}$ (η_P and η_S are the coefficients due to loss) used as a feed signal are together input to the atomic medium again. Before these two fields inject the Raman system, they are subject to respective phase shifts ϕ_1 and ϕ_2 and can be written as $\eta_S \hat{\mathcal{E}}_{S_1} e^{i\phi_1}$ and $\Omega_{P_2} e^{i\phi_2}$. Once they inject the Raman system, the EERS takes place and the propagating quantized Stokes field $\hat{\mathcal{E}}_{S_2}$ obeys the equation of motion [13]

$$\begin{aligned}
(\partial_{t'} + c\partial_z)\hat{\mathcal{E}}_{S_2}(z, t') &= i\chi_2 \hat{S}_{a_2}^\dagger, \\
\partial_{t'} \hat{S}_{a_2}^\dagger &= -\Gamma_{S_2} \hat{S}_{a_2}^\dagger - i\mathcal{W}(t') \chi_2^* \hat{\mathcal{E}}_{S_2} + \hat{F}_{S_2}^\dagger, \quad (14)
\end{aligned}$$

where the subscript 2 of variables $\hat{\mathcal{E}}_{S_2}$, χ_2 , \hat{F}_{S_2} occurs due to the changes $\Omega_{W_1} \rightarrow \Omega_{W_2}$. $\mathcal{W}(t')$ describes the population difference between energy levels $|1\rangle$ and $|2\rangle$ in a short coherence time, which is related to the collective atomic excitation number and the strength of atomic coherence.

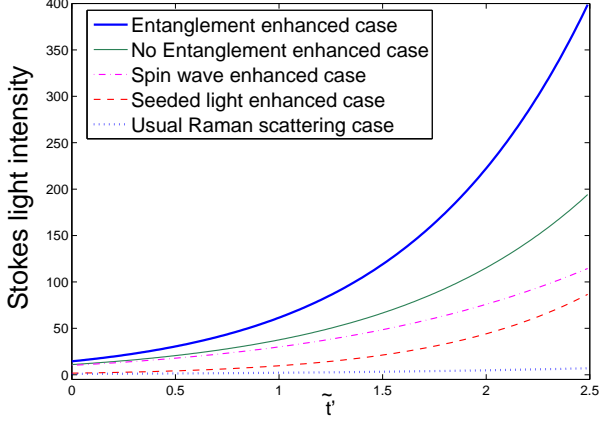


FIG. 3: (Color online) The intensities of Stokes field S_2 versus the dimensionless time t' for URS case (dotted line), seeded light enhanced case (dashed line), spin wave enhanced case (dot-dashed line), no-entanglement enhanced case (thin solid line), and entanglement enhanced case (thick solid line). The parameters are as follows: $\Delta\phi = 0$, $\mathcal{W}(0) = 0.99$, $\eta_P = 0.95$, $\eta_S = 0.9$, $\Delta = 1.2$ GHz, $|\Omega_{P_1}| = 2.5 \times 10^8$ Hz, $Ng^2/c = 1 \times 10^{12}/(m \cdot s)$, $\gamma_s = 10$ KHz, and $\gamma_1 = 2\pi \times 5.746$ MHz.

The form of Eq. (13) is nearly the same as that of Eq. (14) except the population difference $\mathcal{W}(t')$ appearance. In addition, the initial conditions which are used to calculate the Stokes field intensity are different. Although the structure of the equations do not change, the scattering effects are widely different. In the EERS case, different enhanced mechanisms are coherent combining [23], then a strong Raman scattering will be obtained. Next, we give the initial conditions of two cases. In the case of URS, no initial Stokes field is externally incident on the ensemble and no initial spin wave is written into the ensemble, so the initial conditions for the field and spin wave are

$$\langle \hat{\mathcal{E}}_{S_1}^\dagger(0, t') \hat{\mathcal{E}}_{S_1}(0, t') \rangle = 0, \quad \langle \hat{S}_{a_1}^\dagger(z', 0) \hat{S}_{a_1}(z', 0) \rangle = 0. \quad (15)$$

But in the case of the EERS, the generated Stokes field $\hat{\mathcal{E}}_{S_1}$ as a seeded light is injection on the ensemble, so the initial condition for the field $\hat{\mathcal{E}}_{S_2}(0, t')$ is

$$\hat{\mathcal{E}}_{S_2}(0, t') = \hat{\mathcal{E}}_{S_{in}}(t'), \quad \langle \hat{\mathcal{E}}_{S_2}^\dagger(z', 0) \hat{\mathcal{E}}_{S_2}(z', 0) \rangle = 0. \quad (16)$$

Here $\hat{\mathcal{E}}_{S_{in}}(t') = \eta_S \hat{\mathcal{E}}_{S_1}(L, t) e^{i\phi_1}$, and the atomic ensemble contains a spin wave \hat{S}_{a_1} written by the field Ω_{P_1} , so the initial condition for the atomic spin wave $\hat{S}_{a_2}^\dagger(z', 0)$ is

$$\hat{S}_{a_2}^\dagger(z', 0) = \hat{S}_{a_1}^\dagger(L - z', \tau), \quad (17)$$

where $L - z'$ describes two pump fields propagation of opposite direction and τ is the pulse duration of the pump field. Here we neglect the slow decay of the spin wave in the very short delay time.

Using the solutions of Eq. (13) and Eq. (14), the mean intensity of Stokes field at the end of the atomic cell is given by

$$I_{\text{EERS}}(t') = \frac{\hbar\omega_{S_2}c}{L} \langle \hat{\mathcal{E}}_{S_2}^\dagger(L, t') \hat{\mathcal{E}}_{S_2}(L, t') \rangle = I_{\text{spon}_2} + \text{TM}_{\text{seed}} + \text{TM}_{\text{spin-wave}} + \text{TM}_{\text{EPR}}, \quad (18)$$

where

$$\begin{aligned} I_{\text{spon}_2} &= \text{TM}_0, \\ \text{TM}_{\text{seed}} &= \text{TM}_1 + (\text{TM}_2 + \text{c.c.}) + \text{TM}_3, \\ \text{TM}_{\text{spin-wave}} &= \text{TM}_4, \\ \text{TM}_{\text{EPR}} &= (\text{TM}_5 + \text{TM}_6) e^{-i(\phi_1 - \phi_2)} + \text{c.c.} \end{aligned} \quad (19)$$

Here the detailed expressions TM_i ($i = 0, 1, \dots, 6$) are showed in Appendix A. The term TM_0 describes the intensity of Stokes field when only the field P_2 drives the ensemble and no any other enhancement mechanisms existing. When $\mathcal{W}(0) = 1$, this term simplified to the intensity of URS which had been given by Raymer and Mostowski [22]. The terms TM_{seed} , $\text{TM}_{\text{spin-wave}}$, and TM_{EPR} are described as above, i.e., from the seed, spinwave, and entanglement enhancement mechanisms, respectively. Different from above, the propagation effects are included. Next, we analyze the intensity of EERS, and compared it with I_{seed} , $I_{\text{spin-wave}}$, and $I_{\text{no-entangle}}$.

III. ANALYTICAL AND NUMERICAL SOLUTION

Now, we give a simplified expressions of the intensity of Stokes field $\hat{\mathcal{E}}_{S_2}$, and numerically calculate the intensities of the different enhancement mechanisms and compare them with each other. For analyzing conveniently, we assume the pump fields intensity $|E_{P_{1,2}}|^2 [\Omega_{P_{1,2}}(t') = \Omega_{P_{1,2}} \theta(t')]$ being constant and real and switched on at $t' = 0$. For conveniences, we define the dimensionless time $\tilde{t}' = t' \chi_1^2 L/c = t' \chi_2^2 L/(c\eta_P^2)$, $\tilde{\tau} = \tau \chi_1^2 L/c$, therefore the URS term and the enhanced part TM_i ($i = 1, 2, \dots, 6$) under the analytic conditions are rewritten as ATM_i ($i = 1, 2, \dots, 6$) in Appendix B. According to the different scattering mechanisms shown in Fig. 2, the Stokes intensities of different cases can be given as following:

$$\begin{aligned} I_{\text{spon}_2} &= \text{ATM}_0, \\ I_{\text{seed}} &= \text{ATM}_0 + \text{ATM}_1 + 2\text{Re}[\text{ATM}_2] + \text{ATM}_3, \\ I_{\text{spin-wave}} &= \text{ATM}_0 + \text{ATM}_4, \\ I_{\text{no-entangle}} &= I_{\text{seed}} + \text{ATM}_4, \\ I_{\text{EERS}} &= I_{\text{no-entangle}} + 2\text{Re}[\text{ATM}_{\text{ent}}] \cos(\Delta\phi) \\ &\quad + 2\text{Im}[\text{ATM}_{\text{ent}}] \sin(\Delta\phi), \end{aligned} \quad (20)$$

where

$$\text{ATM}_{\text{ent}} = \text{ATM}_5 + \text{ATM}_6, \quad \Delta\phi = \phi_1 - \phi_2. \quad (21)$$

Here the term ATM_{ent} is generated due to the entanglement of the injected Stokes field and the IPSW, and $\Delta\phi$

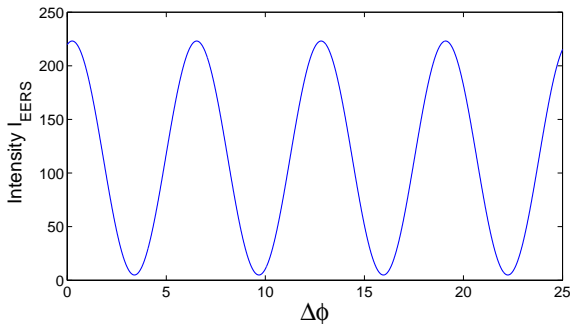


FIG. 4: (Color online) The intensity of Stokes field I_{EERS} versus the relative phase $\Delta\phi$. The other parameters are the same as that of Fig. 3 except the dimensionless time at $\tilde{t}' = 2$.

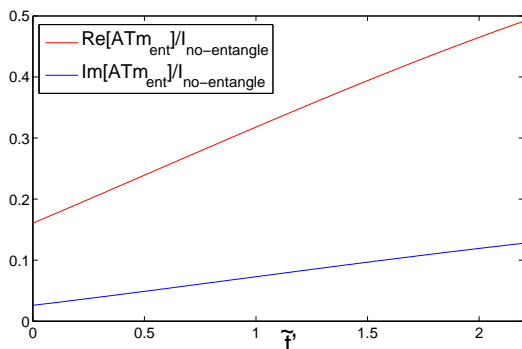


FIG. 5: (Color online) The ratio $\text{Re}[\text{ATm}_{\text{ent}}]/I_{\text{no-entangle}}$ (solid line) and $\text{Im}[\text{ATm}_{\text{ent}}]/I_{\text{no-entangle}}$ (dashed line) versus the dimensionless time \tilde{t}' . The parameters are the same as that of Fig. 3.

is the relative phase between the pump field P_2 and the input seeded light.

In Fig. 3 the intensity of URS case I_{URS} is described by the dotted line where the long time evolution and Raman scattering into steady state is not plotted. As we all know, the Raman scattering intensity will be high when the seeded light injects the atomic medium along with the pumping light, and the dashed line describes the intensity of seeded light enhanced case I_{seed} . The dot-dashed line describes the intensity of spin wave enhanced case $I_{\text{spin-wave}}$. Here the spin wave enhanced case refers to counter-propagation of two pumping fields (P_1 and P_2). As for co-propagation case, only $1 - \tilde{z}$ need to change to \tilde{z} in TM_4 [13]. In Fig. 3, the intensity of spin wave enhanced case $I_{\text{spin-wave}}$ is larger than that of seeded light enhanced case I_{seed} , which is opposited to the results obtained from the few-mode model because the gain coefficients are dependent on the spatial variable \tilde{z} when considering the propagation effects. The effects of spatial coherence on spin wave enhanced Raman scattering has been studied by us in theory and on experiment [8, 9, 13]. The thin solid line (green line) describes the intensity $I_{\text{no-entangle}}$ when the seeded light

is no entangled with another IPSW of the same intensity. If input seeded light is entangled with IPSW, the EERS will be generated. This entanglement enhanced case is phase sensitive and the Stokes intensity is dependent on the relative phase. With $\Delta\phi = 0$, the thick solid line (blue line) describes the intensity of entanglement enhanced case I_{EERS} (see Fig. 3). From the Fig. 3, it is demonstrated that intensity generated by the entanglement enhancement mechanism is the largest of all under a certain relative phase.

We choose a certain dimensionless time at $\tilde{t}' = 2$ and plot the intensity I_{EERS} as a function of the relative phase $\Delta\phi$ shown in Fig. 4. The figure demonstrates that the intensity is modulated by the relative phase $\Delta\phi$. The reason for phase modulation is interference of spin waves. After the first pump field P_1 , the Stokes field and the collective atomic excitation (spin wave) is phase correlated [24]. With the second pump field P_2 , the phase of atomic ensemble is retrieved and interference occurs. From Fig. 5, it is obviously that the imaginary part of the term ATm_{ent} is not only very small but also is far less than the real part of ATm_{ent} at the large time. Therefore the visibility of interference fringe in Fig. 4 is mainly dependent on the real part $\text{Re}[\text{ATm}_{\text{ent}}]$ at the large time. This entanglement enhancement phase sensitive Raman scattering can be used to realize a nonlinear interferometer, where the amplified phase sensing intensity can enhance signal to noise ratio of interferometer [25, 26].

IV. CONCLUSION

In conclusion, we have theoretically studied the entanglement enhanced Raman scattering, which is generated based on the situation that the input seeded light is entangled with the IPSW. Different from other enhancement mechanisms the entanglement enhanced Raman scattering is phase sensitive. The strong enhanced Raman scattering will have practical applications in quantum information, nonlinear optics and optical metrology.

Acknowledgments

This work was supported by the National Basic Research Program of China (973 Program) under Grant No. 2011CB921604 (W.Z.), the National Natural Science Foundation of China under Grant No. 11129402 (Z.Y.O.), No. 11004058, No. 11274118, and Supported by Innovation Program of Shanghai Municipal Education Commission 13zz036 (L.Q.C.), the National Natural Science Foundation of China under Grant No. 11004059 (C.H.Y.).

Email: *zou@iupui.edu; †wpzhang@phy.ecnu.edu.cn

Appendix A: Appendixes

In this Appendix we describe in detail theoretical calculation of the mean intensity of Stokes field $\hat{\mathcal{E}}_{S_2}$ at the

end of the atomic cell. Using the moving coordinates $t' = t - z/c$, $z' = z$, the solution of Eq. (13) is

$$\begin{aligned} \hat{S}_{a_1}^\dagger(z', t') &= e^{-\Gamma_1(t')} \hat{S}_{a_1}^\dagger(z', 0) - i \int_0^{t'} \chi_1(t'') e^{-[\Gamma_1(t') - \Gamma_1(t'')] } H_1(z', 0, t', t'') \hat{\mathcal{E}}_{S_1}(0, t'') dt'' \\ &+ e^{-\Gamma_1(t')} \int_0^{z'} G_{S_1}(z', z'', t', 0) \hat{S}_{a_1}^\dagger(z'', 0) dz'' + \int_0^{t'} e^{-[\Gamma_1(t') - \Gamma_1(t'')] } \hat{F}_{S_1}^\dagger(z', t'') dt'' \\ &+ \int_0^{t'} e^{-[\Gamma_1(t') - \Gamma_1(t'')] } \int_0^{z'} G_{S_1}(z', z'', t', t'') \hat{F}_{S_1}^\dagger(z'', t'') dz'' dt'', \end{aligned} \quad (\text{A1})$$

$$\begin{aligned} \hat{\mathcal{E}}_{S_1}(z', t') &= \hat{\mathcal{E}}_{S_1}(0, t') + \frac{i\chi_1(t')}{c} \int_0^{t'} e^{-[\Gamma_1(t') - \Gamma_1(t'')] } \int_0^{z'} H_1(z', z'', t', t'') \hat{F}_{S_1}^\dagger(z'', t'') dz'' dt'' + \frac{i\chi_1(t')}{c} e^{-\Gamma_1(t')} \\ &\times \int_0^{z'} H_1(z', z'', t', 0) \hat{S}_{a_1}^\dagger(z'', 0) dz'' + \frac{\chi_1(t')}{c} \int_0^{t'} \chi_1(t'') \hat{\mathcal{E}}_{S_1}(0, t'') G_{e_1}(z', 0, t', t'') dt'', \end{aligned} \quad (\text{A2})$$

in which

$$\begin{aligned} H_1(z', z'', t', t'') &= I_0(2\sqrt{[q_1(t') - q_1(t'')] \frac{z' - z''}{c}}), \\ G_{e_1}(z', z'', t', t'') &= \frac{c(z' - z'')}{q_1(t') - q_1(t'')} G_{S_1}(z', z'', t', t''), \\ G_{S_1}(z', z'', t', t'') &= \sqrt{\frac{q_1(t') - q_1(t'')}{c(z' - z'')}} \\ &\times I_1(2\sqrt{[q_1(t') - q_1(t'')] \frac{z' - z''}{c}}), \end{aligned} \quad (\text{A3})$$

where $\Gamma_1(t') = \int_0^{t'} \Gamma_{S_1}(t'') dt''$ and $q_1(t') = \int_0^{t'} \chi_1(t'')^2 dt''$, and $I_n(x)$ is the modified Bessel function of the first kind of order n . This solution is for pencil-shaped atomic ensemble which was given by Ref. [22]. The solutions (A1) and (A2) are used to calculate the mean Stokes intensity and the mean spin wave intensity.

As well, according to Refs. [13, 22], the solution of Eq. (14) is given by

$$\begin{aligned} \hat{S}_{a_2}^\dagger(z', t') &= e^{-\Gamma_2(t')} \hat{S}_{a_2}^\dagger(z', 0) - ie^{-i\phi_2} \int_0^{t'} \mathcal{W}(t'') \chi_2^*(t'') e^{-[\Gamma_2(t') - \Gamma_2(t'')] } H_2(z', 0, t', t'') \hat{\mathcal{E}}_{S_2}(0, t'') dt'' \\ &+ e^{-\Gamma_2(t')} \int_0^{z'} G_{S_2}(z', z'', t', 0) \hat{S}_{a_2}^\dagger(z'', 0) dz'' + \int_0^{t'} e^{-[\Gamma_2(t') - \Gamma_2(t'')] } \hat{F}_{S_2}^\dagger(z', t'') dt'' + \int_0^{t'} e^{-[\Gamma_2(t') - \Gamma_2(t'')] } \\ &\times \int_0^{z'} G_{S_2}(z', z'', t', t'') \hat{F}_{S_2}^\dagger(z'', t'') dz'' dt'', \end{aligned} \quad (\text{A4})$$

$$\begin{aligned} \hat{\mathcal{E}}_{S_2}(z', t') &= \hat{\mathcal{E}}_{S_2}(0, t') + \frac{\chi_2(t')}{c} \int_0^{t'} \mathcal{W}(t'') \chi_2^*(t'') e^{-[\Gamma_2(t') - \Gamma_2(t'')] } \hat{\mathcal{E}}_{S_2}(0, t'') G_{e_2}(z', 0, t', t'') dt'' \\ &+ \frac{i\chi_2(t') e^{i\phi_2}}{c} e^{-\Gamma_2(t')} \int_0^{z'} H_2(z', z'', t', 0) \hat{S}_{a_2}^\dagger(z'', 0) dz'' + \frac{i\chi_2(t') e^{i\phi_2}}{c} \int_0^{t'} e^{-[\Gamma_2(t') - \Gamma_2(t'')] } \\ &\times \int_0^{z'} H_2(z', z'', t', t'') \hat{F}_{S_2}^\dagger(z'', t'') dz'' dt'', \end{aligned} \quad (\text{A5})$$

where

$$H_2(z', z'', t', t'') = I_0(2\sqrt{[q_2(t') - q_2(t'')] \frac{z' - z''}{c}}),$$

$$G_{e_2}(z', z'', t', t'') = \frac{c(z' - z'')}{q_2(t') - q_2(t'')} G_{S_2}(z', z'', t', t''),$$

$$\begin{aligned}
G_{S_2}(z', z'', t', t'') &= \sqrt{\frac{q_2(t') - q_2(t'')}{c(z' - z'')}} \\
&\times I_1(2\sqrt{[q_2(t') - q_2(t'')] \frac{z' - z''}{c}}), \\
\mathcal{W}(t) &= \mathcal{W}(0)e^{-\Gamma_2'(t)} - \int_0^t \gamma_2'(t')e^{-[\Gamma_2'(t) - \Gamma_2'(t')]} dt'.
\end{aligned} \tag{A6}$$

Here $\langle \hat{F}_{S_2}(z, t) \hat{F}_{S_2}^\dagger(z', t') \rangle = 2\gamma_{S_2} L \delta(z - z') \delta(t - t')$,
 $\Gamma_2(t') = \int_0^{t'} \Gamma_{S_2}(t'') dt''$, $q_2(t') = \int_0^{t'} \mathcal{W}(t'') |\chi_2(t'')|^2 dt''$,
 $\chi_2(z, t) = g\sqrt{N}\Omega_{P_2}(z, t)/\Delta$, $\Gamma_2'(t') = \int_0^{t'} \gamma_2'(t'') dt''$,
 $\Gamma_{S_2} = \gamma_{S_2} - i|\Omega_{P_2}|^2/\Delta$, $\gamma_{S_2} = \gamma_{S_0} + \gamma_1|\Omega_{P_2}|^2/\Delta^2$,
 $\gamma_2' = \gamma_1|\Omega_{P_2}|^2/\Delta^2$, γ_{S_0} the coherence ($\tilde{\sigma}_{12}$) decay rate,

γ_1 the decay rates of the excited state |3) to states |1) and |2) (assuming $\gamma_{31} = \gamma_{32} = \gamma_1$). The small population differences $\mathcal{W}(0) = \tilde{\sigma}_{11}(0) - \tilde{\sigma}_{22}(0)$ and $\mathcal{W}(t)$ generated by the respective pump fields P_1 and P_2 . The small population difference $\mathcal{W}(t)$ only describes the population change of a short time.

Using Eqs. (A1)-(A2) and Eqs. (A5)-(A5), the mean intensity at the end of the atomic cell is given by

$$I_{\text{EERS}}(t') = \frac{\hbar\omega_{S_2}c}{L} \langle \hat{\mathcal{E}}_{S_2}^\dagger(L, t') \hat{\mathcal{E}}_{S_2}(L, t') \rangle = \sum_{j=0}^6 \text{TM}_j, \tag{A7}$$

where

$$\begin{aligned}
\text{TM}_0 &= \frac{\hbar\omega_{S_2} |\chi_2(t')|^2 L}{c} e^{-2\text{Re}[\Gamma_2(t')]} \left\{ \int_0^1 \left| I_0(2\sqrt{Q_2(t')(1-\tilde{z})}) \right|^2 d\tilde{z} \right. \\
&\quad \left. + 2\gamma_{S_2} \int_0^{t'} dt'' e^{2\text{Re}[\Gamma_2(t'')]} \int_0^1 \left| I_0(2\sqrt{(Q_2(t') - P_2(t''))(1-\tilde{z})}) \right|^2 d\tilde{z} \right\},
\end{aligned} \tag{A8}$$

$$\begin{aligned}
\text{TM}_1 &= \frac{\hbar\omega_{S_2}c}{L} \langle \hat{\mathcal{E}}_{S_2}^\dagger(0, t') \hat{\mathcal{E}}_{S_2}(0, t') \rangle = \eta_S^2 \frac{\hbar\omega_{S_2} |\chi_1(t')|^2}{c} e^{-2\text{Re}[\Gamma_1(t')]} \left\{ \int_0^1 \left| I_0(2\sqrt{Q_1(t')(1-\tilde{z})}) \right|^2 d\tilde{z} \right. \\
&\quad \left. + 2\gamma_{S_1} \int_0^{t'} dt'' e^{2\text{Re}[\Gamma_1(t'')]} \int_0^1 \left| I_0(2\sqrt{(Q_1(t') - Q_1(t''))(1-\tilde{z})}) \right|^2 d\tilde{z} \right\},
\end{aligned} \tag{A9}$$

$$\begin{aligned}
\text{TM}_2 &= \frac{\hbar\omega_{S_2}\chi_2(t')}{L} \int_0^{t'} \mathcal{W}(t'') \chi_2^*(t'') e^{-[\Gamma_2(t') - \Gamma_2(t'')]} \langle \hat{\mathcal{E}}_{S_2}^\dagger(0, t') \hat{\mathcal{E}}_{S_2}(0, t'') \rangle G_{e_2}(L, 0, t', t'') dt'' \\
&= \eta_S^2 \frac{\hbar\omega_{S_2}\chi_1^*(t')\chi_2(t')L^2}{c^2} e^{-\Gamma_1^*(t')} e^{-\Gamma_2(t')} \int_0^{t'} dt'' e^{-\Gamma_1(t'')} e^{\Gamma_2(t'')} \mathcal{W}(t'') \chi_1(t'') \chi_2^*(t'') G_{E_2}(t', t'') \\
&\quad \times \{Fint(t', t'') + 2\gamma_{S_1} \int_0^{t'} e^{2\text{Re}[\Gamma_1(t''')] } Fint(t' - t''', t'' - t''') dt'''\},
\end{aligned} \tag{A10}$$

$$\begin{aligned}
\text{TM}_3 &= \frac{\hbar\omega_{S_2} |\chi_2(t')|^2}{Lc} e^{-2\text{Re}[\Gamma_2(t')]} \int_0^{t'} e^{\Gamma_2^*(t'')} \mathcal{W}(t'') \chi_2(t'') G_{e_2}^*(L, 0, t', t'') dt'' \\
&\quad \times \int_0^{t'} e^{\Gamma_2(t''')} \mathcal{W}(t''') \chi_2^*(t''') G_{e_2}(L, 0, t', t''') dt''' \langle \hat{\mathcal{E}}_{S_2}^\dagger(0, t') \hat{\mathcal{E}}_{S_2}(0, t''') \rangle \\
&= \eta_S^2 \frac{\hbar\omega_{S_2} |\chi_2(t')|^2 L^3}{c^3} e^{-2\text{Re}[\Gamma_2(t')]} \int_0^{t'} e^{\Gamma_2^*(t'')} e^{-\Gamma_1^*(t'')} \mathcal{W}(t'') \chi_1^*(t'') \chi_2(t'') G_{E_2}^*(t', t'') dt'' \int_0^{t'} dt''' e^{\Gamma_2(t''')} e^{-\Gamma_1(t''')} \\
&\quad \times \mathcal{W}(t''') \chi_1(t''') \chi_2^*(t''') G_{E_2}(t', t''') \{Fint(t'', t''') + 2\gamma_{S_1} \int_0^{t'''} e^{2\text{Re}[\Gamma_1(t'''')] } Fint(t'' - t'''', t''' - t'''') dt''''\},
\end{aligned} \tag{A11}$$

$$\begin{aligned}
\text{TM}_4 &= \frac{\hbar\omega_{S_2} |\chi_2(t')|^2}{Lc} e^{-2\text{Re}[\Gamma_2(t')]} \int_0^L H_2^*(L, z', t', 0) dz' \int_0^L H_2(L, z'', t', 0) \langle \hat{S}_{a_2}^\dagger(z'', 0) \hat{S}_{a_2}(z', 0) \rangle dz'' \\
&= \frac{\hbar\omega_{S_2} |\chi_2(t')|^2 L}{c} e^{-2\text{Re}[\Gamma_2(t')]} \int_0^1 \left| I_0(2\sqrt{P_2(t')(1-\tilde{z})}) \right|^2 n(1-\tilde{z}, \tau) d\tilde{z},
\end{aligned} \tag{A12}$$

$$\begin{aligned}
\text{TM}_5 &= e^{i\phi_2} \frac{i\hbar\omega_{S_2}\chi_2(t')}{L} e^{-\Gamma_2(t')} \int_0^L H_2(L, z'', t', 0) \langle \hat{\mathcal{E}}_{S_2}^\dagger(0, t') \hat{S}_{a_2}^\dagger(z'', 0) \rangle dz'' \\
&= e^{-i(\phi_1 - \phi_2)} \eta_S \frac{\hbar\omega_{S_2}\chi_1^*(t')\chi_2(t')L}{c} e^{-\Gamma_1^*(t') - \Gamma_2(t')} \int_0^1 d\tilde{z} I_0(2\sqrt{P_2(t')(1-\tilde{z})}) \times \{e^{-\Gamma_1(t')} [I_0(2\sqrt{P_1(t')\tilde{z}})]^* \\
&\quad + 2\gamma_{S_1} \int_0^{t'} e^{2\text{Re}[\Gamma_1(t'')]} I_0(2\sqrt{(Q_1(t') - Q_1(t''))\tilde{z}})^* dt''\} + e^{-\Gamma_1(\tau)} [2\gamma_{S_1} \int_0^{t'} dt'' \sqrt{\frac{Q_1(\tau) - Q_1(t'')}{1-2\tilde{z}}} \\
&\quad \times I_1(2\sqrt{(Q_1(\tau) - Q_1(t''))(1-2\tilde{z})}) \int_0^1 I_0(2\sqrt{(Q_1(t') - Q_1(t''))(1-\tilde{z}')})^* d\tilde{z}' \\
&\quad + \int_0^1 \sqrt{\frac{Q_1(\tau)}{1-\tilde{z}-\tilde{z}'}} I_1(2\sqrt{Q_1(\tau)(1-\tilde{z}-\tilde{z}')} I_0(2\sqrt{Q_1(t')(1-\tilde{z}')})^* d\tilde{z}']\}, \tag{A13}
\end{aligned}$$

$$\begin{aligned}
\text{TM}_6 &= e^{i\phi_2} \frac{i\hbar\omega_{S_2} |\chi_2(t')|^2}{Lc} e^{-2\text{Re}[\Gamma_2(t')]} \int_0^{t'} e^{\Gamma_2^*(t'')} \mathcal{W}(t'') \chi_2^*(t'') G_{e_2}^*(L, 0, t', t'') dt'' \\
&\quad \times \int_0^L H_2(L, z'', t', 0) \langle \hat{\mathcal{E}}_{S_2}^\dagger(0, t'') \hat{S}_{a_2}^\dagger(z'', 0) \rangle dz'' \\
&= e^{-i(\phi_1 - \phi_2)} \eta_S \frac{\hbar\omega_{S_2}\chi_1^*(t') |\chi_2(t')|^2 L^2}{c^2} e^{-2\text{Re}[\Gamma_2(t')]} \int_0^{t'} dt'' e^{\Gamma_2^*(t'')} \mathcal{W}(t'') \chi_2(t'') G E_2^*(t', t'') \\
&\quad \times \int_0^1 d\tilde{z} I_0(2\sqrt{Q_2(t')(1-\tilde{z})}) \{e^{-2\text{Re}[\Gamma_1(t'')]} [I_0(2\sqrt{Q_1(t'')\tilde{z}})]^* + 2\gamma_{S_1} \int_0^{t''} e^{2\text{Re}[\Gamma_1(t''')]} \\
&\quad \times I_0(2\sqrt{(Q_1(t'') - Q_1(t'''))\tilde{z}})^* dt'''\} + e^{-\Gamma_1(\tau)} e^{-\Gamma_1^*(t'')} \\
&\quad \times [\int_0^1 \sqrt{\frac{Q_1(\tau)}{1-\tilde{z}-\tilde{z}'}} I_1(2\sqrt{Q_1(\tau)(1-\tilde{z}-\tilde{z}')} I_0(2\sqrt{Q_1(t'')(1-\tilde{z}')})^* d\tilde{z}' \\
&\quad + 2\gamma_{S_1} \int_0^{t''} \sqrt{\frac{Q_1(\tau) - Q_1(t''')}{1-2\tilde{z}}} I_1(2\sqrt{(Q_1(\tau) - Q_1(t'''))(1-2\tilde{z})}) dt'''\} \\
&\quad \times \int_0^1 I_0(2\sqrt{(Q_1(t'') - Q_1(t'''))(1-\tilde{z}')})^* d\tilde{z}']\}, \tag{A14}
\end{aligned}$$

and

$$\begin{aligned}
G E_2(t', t'') &= \frac{I_1(2\sqrt{Q_2(t') - Q_2(t'')})}{\sqrt{Q_2(t') - Q_2(t'')}}, \\
n(\tilde{z}, \tau) &= \frac{L}{c} e^{-2\text{Re}[\Gamma_1(\tau)]} \int_0^\tau e^{2\text{Re}[\Gamma_1(t'')]} |\chi_1(t'')|^2 \left| I_0(2\sqrt{(Q_1(\tau) - Q_1(t''))(1-\tilde{z})}) \right|^2 dt'', \\
F_{\text{int}}(t', t'') &= \int_0^1 I_0(2\sqrt{Q_1(t')(1-\tilde{z})})^* I_0(2\sqrt{Q_1(t'')(1-\tilde{z})}) d\tilde{z}, \\
F_{\text{int}}(t' - t''', t'' - t''') &= \int_0^1 I_0(2\sqrt{(Q_1(t') - Q_1(t'''))(1-\tilde{z})})^* \\
&\quad \times I_0(2\sqrt{(Q_1(t'') - Q_1(t'''))(1-\tilde{z})}) d\tilde{z}, \\
Q_1(t') &= \frac{q_1(t')L}{c}, \quad Q_2(t') = \frac{q_2(t')L}{c}. \tag{A15}
\end{aligned}$$

Here, the slowly varying electric field commutation relation $[\hat{\mathcal{E}}_{S_1}(z, t), \hat{\mathcal{E}}_{S_1}^\dagger(z, t')] = \frac{L}{c} \delta(t - t')$ and the spin wave

commutation relation $[\hat{S}_{a_1}(z, t), \hat{S}_{a_1}^\dagger(z', t)] = L\delta(z - z')$

are used. Terms TM_1 , TM_2 and TM_3 are generated due to the input the seeded Stokes field. Note that for $\eta_S = 1$, the first term TM_1 is the input intensity of the Stokes field $I_{S_1}(t') = \hbar\omega_{S_2}c/L\langle\hat{\mathcal{E}}_{S_2}^\dagger(0, t')\hat{\mathcal{E}}_{S_2}(0, t')\rangle$. The term TM_4 ($\text{TM}_{\text{spin-wave}}$) is generated by spin wave enhancement mechanism which has been studied by us [8, 13]. Here the spin wave enhanced case refers to counter-propagation of two pumping fields. As for co-propagation case, only $1 - \tilde{z}$ need to change to \tilde{z} in TM_4 [13]. Terms TM_5 and TM_6 are generated by the correlation of the feed field and the polarization field.

Appendix B: Appendix

Next, we consider the pump fields intensity being constant and real, after being switched on $t' = 0$, so $\Gamma_{1,2}(t') = \Gamma_{S_{1,2}}t'$, $q_1(t') = \chi_1^2 t'$, $q_2(t') = \eta(t')\chi_2^2 t'$, $\eta(t') = \mathcal{W}(0)(1 - 1/(2\gamma_2' t')) - 1/(2\gamma_2' t')$. Using the dimensionless time \tilde{t}' , then the above terms TM_i ($i = 1, 2, \dots, 6$) can be rewritten as ATM_i and are given by

$$\begin{aligned} \text{ATM}_0 &= \eta_P^2 \frac{\hbar\omega_{S_2}\chi_1^2 L}{c} e^{-2\gamma_{S_2}c\tilde{t}'/\chi_1^2 L} \left\{ I_0 \left(2\eta_P \sqrt{\eta(\tilde{t}')\tilde{t}'} \right)^2 - I_1 \left(2\eta_P \sqrt{\eta(\tilde{t}')\tilde{t}'} \right)^2 \right. \\ &\quad \left. + \frac{2\gamma_{S_2}c}{\chi_1^2 L} \int_0^{\tilde{t}'} e^{2\gamma_{S_2}c\tilde{t}''/\chi_1^2 L} \left[I_0 \left(2\eta_P \sqrt{\eta(\tilde{t}')\tilde{t}'} - \eta(\tilde{t}'')\tilde{t}'' \right)^2 - I_1 \left(2\eta_P \sqrt{\eta(\tilde{t}')\tilde{t}'} - \eta(\tilde{t}'')\tilde{t}'' \right)^2 \right] d\tilde{t}'' \right\}, \end{aligned} \quad (\text{B1})$$

$$\begin{aligned} \text{ATM}_1 &= \eta_S^2 \frac{\hbar\omega_{S_2}\chi_1^2 L}{c} e^{-2\gamma_{S_1}c\tilde{t}'/\chi_1^2 L} \left\{ I_0 \left(2\sqrt{\tilde{t}'} \right)^2 - I_1 \left(2\sqrt{\tilde{t}'} \right)^2 \right. \\ &\quad \left. + \frac{2\gamma_{S_1}c}{\chi_1^2 L} \int_0^{\tilde{t}'} e^{2\gamma_{S_1}c\tilde{t}''/\chi_1^2 L} \left[I_0 \left(2\sqrt{\tilde{t}'} - \tilde{t}'' \right)^2 - I_1 \left(2\sqrt{\tilde{t}'} - \tilde{t}'' \right)^2 \right] d\tilde{t}'' \right\}, \end{aligned} \quad (\text{B2})$$

$$\begin{aligned} \text{ATM}_2 &= \eta_S^2 \eta_P^2 \frac{\hbar\omega_{S_2}\chi_1^2 L}{c} e^{-\frac{(\Gamma_{S_1}^* + \Gamma_{S_2})c\tilde{t}'}{\chi_1^2 L}} \int_0^{\tilde{t}'} d\tilde{t}'' e^{-(\Gamma_{S_1} - \Gamma_{S_2})c\tilde{t}''/\chi_1^2 L} \mathcal{W}(\tilde{t}'') \text{GE}2(\tilde{t}', \tilde{t}'') \{ \text{Fint}(\tilde{t}', \tilde{t}'') \\ &\quad + 2 \frac{\gamma_{S_1}c}{\chi_1^2 L} \int_0^{\tilde{t}'} e^{\frac{2\gamma_{S_1}c\tilde{t}'''}{\chi_1^2 L}} \text{Fint}(\tilde{t}' - \tilde{t}''', \tilde{t}'' - \tilde{t}''') d\tilde{t}''' \}, \end{aligned} \quad (\text{B3})$$

$$\begin{aligned} \text{ATM}_3 &= \eta_S^2 \eta_P^4 \frac{\hbar\omega_{S_2}\chi_1^2 L}{c} e^{-2\gamma_{S_2}c\tilde{t}'/\chi_1^2 L} \int_0^{\tilde{t}'} e^{\frac{(\Gamma_{S_2}^* - \Gamma_{S_1}^*)c\tilde{t}''}{\chi_1^2 L}} \mathcal{W}(\tilde{t}'') \text{GE}2(\tilde{t}', \tilde{t}'') d\tilde{t}'' \int_0^{\tilde{t}'} d\tilde{t}''' e^{\frac{(\Gamma_{S_2} - \Gamma_{S_1})c\tilde{t}'''}{\chi_1^2 L}} \mathcal{W}(\tilde{t}''') \text{GE}2(\tilde{t}', \tilde{t}''') \\ &\quad \times \{ \text{Fint}(\tilde{t}', \tilde{t}''') + \frac{2\gamma_{S_1}c}{\chi_1^2 L} \int_0^{\tilde{t}'''} e^{\frac{2\gamma_{S_1}c\tilde{t}''''}{\chi_1^2 L}} \text{Fint}(\tilde{t}'' - \tilde{t}'''', \tilde{t}''' - \tilde{t}''') d\tilde{t}'''' \}, \end{aligned} \quad (\text{B4})$$

$$\text{ATM}_4 = \eta_P^2 \frac{\hbar\omega_{S_2}\chi_1^2 L}{c} e^{-2\gamma_{S_2}c\tilde{t}'/\chi_1^2 L} \int_0^1 I_0 \left(2\eta_P \sqrt{\eta(\tilde{t}')\tilde{t}'(1 - \tilde{z})} \right)^2 n(1 - \tilde{z}, \tilde{\tau}) d\tilde{z}, \quad (\text{B5})$$

$$\begin{aligned} \text{ATM}_5 &= e^{-i(\phi_1 - \phi_2)} \eta_S \eta_P \frac{\hbar\omega_{S_2}\chi_1^2 L}{c} e^{-(\Gamma_{S_1}^* + \Gamma_{S_2})c\tilde{t}'/\chi_1^2 L} \int_0^1 d\tilde{z} I_0(2\eta_P \sqrt{\eta(\tilde{t}')\tilde{t}'(1 - \tilde{z})}) \{ e^{-\frac{\Gamma_{S_1}c\tilde{t}'}{\chi_1^2 L}} [I_0(2\sqrt{\tilde{t}'\tilde{z}}) \\ &\quad + 2 \frac{\gamma_{S_1}c}{\chi_1^2 L} \int_0^{\tilde{t}'} e^{\frac{2\gamma_{S_1}c\tilde{t}''}{\chi_1^2 L}} I_0(2\sqrt{(\tilde{t}' - \tilde{t}'')\tilde{z}}) d\tilde{t}''] + e^{-\frac{\Gamma_{S_1}c\tilde{t}'}{\chi_1^2 L}} [\int_0^1 G_{S_1}(1 - \tilde{z}, \tilde{z}', \tilde{\tau}, 0) I_0(2\sqrt{\tilde{t}'(1 - \tilde{z}')}) d\tilde{z}' \\ &\quad + 2 \frac{\gamma_{S_1}c}{\chi_1^2 L} \int_0^{\tilde{t}'} G_{S_1}(1 - \tilde{z}, \tilde{z}, \tilde{\tau}, \tilde{t}'') d\tilde{t}'' \int_0^1 I_0(2\sqrt{(\tilde{t}' - \tilde{t}'')(1 - \tilde{z}')}) d\tilde{z}'] \}, \end{aligned} \quad (\text{B6})$$

$$\begin{aligned} \text{ATM}_6 &= e^{-i(\phi_1 - \phi_2)} \eta_S \eta_P^3 \frac{\hbar\omega_{S_2}\chi_1^2 L}{c} e^{-\frac{2\gamma_{S_2}c\tilde{t}'}{\chi_1^2 L}} \int_0^{\tilde{t}'} d\tilde{t}'' e^{\frac{\Gamma_{S_2}^*c\tilde{t}''}{\chi_1^2 L}} \mathcal{W}(\tilde{t}'') \text{GE}_2(\tilde{t}', \tilde{t}'') \int_0^1 d\tilde{z} I_0(2\eta_P \sqrt{\eta(\tilde{t}')\tilde{t}''(1 - \tilde{z})}) \{ e^{-\frac{2\gamma_{S_1}c\tilde{t}''}{\chi_1^2 L}} \\ &\quad \times [I_0(2\sqrt{\tilde{t}'\tilde{z}}) + 2 \frac{\gamma_{S_1}c}{\chi_1^2 L} \int_0^{\tilde{t}'} e^{\frac{2\gamma_{S_1}c\tilde{t}'''}{\chi_1^2 L}} I_0(2\sqrt{(\tilde{t}' - \tilde{t}''')\tilde{z}}) d\tilde{t}'''] + e^{-\frac{\Gamma_{S_1}c\tilde{t}'' + \Gamma_{S_1}^*c\tilde{t}''}{\chi_1^2 L}} [\int_0^1 d\tilde{z}' G_{S_1}(1 - \tilde{z}, \tilde{z}', \tilde{\tau}, 0) \\ &\quad \times I_0(2\sqrt{\tilde{t}'(1 - \tilde{z}')}) + 2 \frac{\gamma_{S_1}c}{\chi_1^2 L} \int_0^{\tilde{t}'} G_{S_1}(1 - \tilde{z}, \tilde{z}, \tilde{\tau}, \tilde{t}'') d\tilde{t}'' \int_0^1 I_0(2\sqrt{(\tilde{t}' - \tilde{t}'')(1 - \tilde{z}')}) d\tilde{z}'] \}, \end{aligned} \quad (\text{B7})$$

where

$$n(\tilde{z}) = \int_0^{\tilde{\tau}} e^{-2\gamma_{S_1}c\tilde{t}'/\chi_1^2 L} I_0 \left(2\sqrt{\tilde{t}'\tilde{z}} \right)^2 d\tilde{t}',$$

$$G_{S_1}(\tilde{z}', \tilde{z}'', \tilde{t}', \tilde{t}'') = \sqrt{\frac{\tilde{t}' - \tilde{t}''}{\tilde{z}' - \tilde{z}''}} I_1 \left(2\sqrt{(\tilde{t}' - \tilde{t}'')(\tilde{z}' - \tilde{z}'')} \right),$$

$$\begin{aligned} \text{Fint}(\tilde{t}', \tilde{t}'') &= I_0(2\sqrt{\tilde{t}'})^2 - I_1(2\sqrt{\tilde{t}'})^2, \quad \text{if } \tilde{t}' = \tilde{t}'', \\ \text{Fint}(\tilde{t}', \tilde{t}'') &= \frac{1}{\tilde{t}' - \tilde{t}''} [\sqrt{\tilde{t}'} I_0(2\sqrt{\tilde{t}''}) I_1(2\sqrt{\tilde{t}'}) \\ &\quad - \sqrt{\tilde{t}''} I_0(2\sqrt{\tilde{t}'}) I_1(2\sqrt{\tilde{t}''})], \quad \text{if } \tilde{t}' \neq \tilde{t}''. \end{aligned} \quad (\text{B8})$$

-
- [1] R. H. Dicke, Phys. Rev. **93**, 99 (1954).
- [2] M. Jain, H. Xia, G. Y. Yin, A. J. Merriam, and S.E.Harris, Phys. Rev. Lett. **77**, 4326 (1996).
- [3] A. T. Black, James K. Thompson, and Vladan Vuletić, Phys. Rev. Lett. **95**, 133601 (2005).
- [4] J. Simon, H. Tanji, J. K. Thompson, V. Vuletić, Phys. Rev. Lett. **98**, 183601 (2007).
- [5] J. Simon, H. Tanji, S. Ghosh, and V. Vuletić, Nature Phys. **3**, 765 (2007).
- [6] M. O. Scully, and A. A. Svidzinsky, Science **325**, 1510 (2009); *ibid.* **328**, 1239 (2010).
- [7] E. A. Sete, A. A. Svidzinsky, H. Eleuch, Z. Yang, R. D. Nevels, and M. O. Scully, J. Mod. Opt. **57**, 1311 (2010).
- [8] L. Q. Chen, G. W. Zhang, Chun-Hua Yuan, J. T. Jing, Z. Y. Ou, and W. P. Zhang, Appl. Phys. Lett. **95**, 041115 (2009).
- [9] L. Q. Chen, Guo-Wan Zhang, Cheng-ling Bian, Chun-Hua Yuan, Z. Y. Ou, and Weiping Zhang, Phys. Rev. Lett. **105**, 133603 (2010).
- [10] G. S. Agarwal, Phys. Rev. A **83**, 023802 (2011); R. Wiegner, J. von Zanthier, and G. S. Agarwal, Phys. Rev. A **84**, 023805 (2011).
- [11] M. D. Lukin, P. R. Hemmer, and M. O. Scully, Adv. At., Mol., Opt. Phys. **42**, 347 (2000).
- [12] R. W. Boyd, Nonlinear Optics (Academic Press, San Diego, 1992).
- [13] Chun-Hua Yuan, L. Q. Chen, J. T. Jing, Z. Y. Ou, and W. P. Zhang, Phys. Rev. A **82**, 013817 (2010).
- [14] M. G. Raymer, J. Mod. Opt. **51**, 1739 (2004);
- [15] W. Wasilewski, M. G. Raymer, Phys. Rev. A **73**, 063816 (2006).
- [16] W. Ji, C. Wu, S. J. van Enk, and M. G. Raymer **75**, 052305 (2007).
- [17] A. Einstein, B. Podolsky, and N. Rosen, Phys. Rev. **47**, 777 (1935).
- [18] Z. Y. Ou, S. F. Pereira, H. J. Kimble and K. C. Peng, Phys. Rev. Lett. **68**, 3663 (1992).
- [19] K. Banaszek, K. Wódkiewicz, Acta Phys. Slovaca **49**, 491 (1999).
- [20] The interaction between the forward-scattered light mode and the atoms is described by the Hamiltonian $\hat{H} = \hbar(\sqrt{N}\Omega g/\Delta)\hat{a}^\dagger\hat{S}^\dagger + \text{H.c.}$. Before Raman scattering, the Raman mode and the atomic spin mode are in the vacuum state $|0\rangle_{\text{photon}}|0\rangle_{\text{spin}}$. After the classical drive field, the system coherent evolves from the vacuum state to a two-mode squeezed state $|\psi\rangle = \sum_0^\infty c_n|n\rangle_{\text{photon}}|n\rangle_{\text{spin}}$, where c_n is probability amplitudes.
- [21] D. F. Walls and G. J. Milburn, Quantum Optics (Springer-Verlag, Berlin, 1995).
- [22] M. G. Raymer, and J. Mostowski, Physical Review A **24**, 1980 (1981).
- [23] D. Sabourdy, V. Kermene, A. Desfarges-Berthelebot, L. Lefort, A. Barthelemy, P. Even, and D. Pureur, Opt. Express **11**, 87 (2003).
- [24] Cheng-ling Bian, L. Q. Chen, Guo-Wan Zhang, Z. Y. Ou, Weiping Zhang, Europhys. Lett. **97**, 34005 (2012).
- [25] B. Yurke, S. L. McCall, and J. R. Klauder, Phys. Rev. A **33**, 4033 (1985).
- [26] J. T. Jing, C. J. Liu, Z. F. Zhou, Z. Y. Ou, and W. P. Zhang, Appl. Phys. Lett. **99**, 011110 (2011).